Multi-energy SXR imaging diagnostics for fusion experiments

D. Stutman[1], K. Tritz[1], D. J. Clayton[1], D. Kumar[1], M. Finkenthal[1], R. Bell[2], B. LeBlanc[2]

[1]*Johns Hopkins University, Baltimore, USA*

[2]*Princeton University, Princeton, USA*

New spectroscopic diagnostic designs are needed for future fusion experiments, capable covering a broad energy range with good space and time resolution and being able to survive the fusion environment for long periods of time. The JHU group is developing a multi-energy diagnostic (ME-SXR) in which filtered detector arrays measure the SXR plasma profiles with high space/time resolution but coarse energy discrimination [1], while a transmission grating imaging spectrometer (TGIS) measures the EUV impurity line emission with higher spectral resolution but lower space/time resolution [2]. The space resolved TGIS spectra enable accurate modelling of the ME-SXR data or can be used for standalone impurity monitoring, from low-Z elements such as Li, to high-Z ones such as W. Experiments on NSTX showed that this diagnostic combination enables measuring with good accuracy, speed and spatial resolution the impurity content, impurity transport and the T_e profiles from the core to the edge plasma [1-6]. Spectroscopic techniques for fast T_e profile measurements are important in the ST because ECE is not applicable at low field. In this paper we focus on the potential of the ME-SXR and TGIS for divertor diagnostic and for non-magnetic plasma sensing, including possible burning plasma application.

The principle of the ME-SXR measurement is simple (Fig.1a). Several 1-D pinhole cameras consisting of a slit, a foil filter and a linear detector array are stacked so that they view with good approximation the same plasma volume. We tested as detectors 'optical' arrays consisting of an X-ray phosphor followed by a PMT array or an image intensifier [4,5], as well as absolute XUV photodiode arrays followed by current amplifiers [7]. The optical detector has the advantage of high immunity to EM noise and nuclear radiation background, while the diode one that of high dynamic range and accurately known spectral response. The filters are chosen such that the cutoff energies are roughly multiples of the expected line-of-sight temperature [5]. In addition, the filter material and thickness can be tuned to discriminate specific features in the plasma spectrum, such as the M, L and K-shell emission of iron in Fig. 1b for instance [5,7].

The principle of measuring the plasma SXR emission in multiple energy bands can be applied using also energy-resolving detectors, such as Si or gas photon counters. Pixilated Si photon counters are envisioned for instance for spectrally resolved X-ray imaging of the ITER core [8]. The filtered ME-SXR diagnostic has nevertheless specific advantages. First, it can be applied to colder plasmas regions such as the edge or the divertor, where the energy of the photons is too low for energy-resolving detectors. Secondly, it can measure the SXR emission with much higher speed than possible with photon counters (<1 kHz), enabling for instance measurement of T_e perturbations associated with fast (>10 kHz) MHD modes [7]. Lastly, due to their robustness and relative noise immunity, the ME-SXR arrays can be placed close to the plasma or even in-vessel, enabling to access plasma regions difficult to view with remotely placed sensitive detectors, such as the pedestal.

The ME-SXR measurements at NSTX successfully progressed from the core [4-6] to the edge plasma [1,7]. A system of toroidally displaced tangential ME-SXR arrays is also planned for NSTX-Upgrade aimed at discriminating n>0 emissivity perturbations, such as produced by RWM or by 3-D fields, from toroidally symmetric equilibrium changes [5].

The question thus arises if the multi-energy diagnostic could be extended even further, to the colder divertor plasma. A useful measurement in NSTX would be for instance mapping T_e in the divertor. While the spectroscopic T_e diagnostic cannot rival the accuracy of Thomson scattering it would have nevertheless the advantage of being much simpler and less costly to implement, in particular since in the divertor a 2-D T_e measurements is desirable.

The divertor plasma is characterized by a large variation in the electron temperature, from a few eV near the divertor plates, to around 100 eV near the main plasma. Since such temperatures are difficult to measure using the slope of the SXR continuum, the method we consider for multi-energy divertor T_e diagnostic is measuring with moderate energy resolution, but over a wide spectral range, the pattern of line emission from intrinsic and seeded impurities. This method is illustrated in Fig. 2a, which plots the power emitted by a D plasma having 4% C and 0.8% Ne, in the spectral range from 0 to 1500 Å (labeled 'VUV') and from 0 to 150 Å (labeled 'SXR'). The electron temperature ranges from 25 to 200 eV and the spectra are binned in 100 Å and 10 Å intervals respectively, simulating a low resolution multi-energy diagnostic. As seen, the low resolution but spectrally broad emission patterns contain sufficient information to enable both attributing a unique temperature to each pattern and identifying the main impurities and charge states.

The multi-energy device proposed for such measurements is sketched in Fig. 2a and consists of a dual TGIS spectrometer having transmission gratings covering the above spectral ranges. As shown in Ref. 2, the TGIS works equally well in the SXR and the VUV, since the diffraction efficiency of a free-standing transmission grating is practically independent of its period. The detector can be a MgF_2 MCP intensifier, or for best performance, a direct detection XUV CCD. The device in Fig. 2 would be simple and compact enough to enable implementing two such diagnostics with orthogonal views, for two-dimensional T_e mapping in the NSTX divertor.

Further on we examine the potential of the ME-SXR for non-magnetic plasma sensing. Non-magnetic sensing could be important for the control of long pulse devices such as ITER or FAST, where due to the long time scales dB/dt can be difficult to measure. Important issues are for instance detecting type-I ELMs or RWM instabilities in order to trigger the active control system, or detecting with high sensitivity the L-H transition [8].

The NSTX data suggests that the ME-SXR diagnostic has high potential in this respect. Fig. 3a plots for instance the 'high' (E>1.4 keV) and 'low' energy (E>0.4 keV) ME-SXR profiles measured during type-I ELMS in NSTX. As seen, while the low-E emission profile is little changed by the ELM, the high-E emission profile has high values inside the pedestal before the ELM, crashing to low values after. The 'ME-SXR temperature' at r/a=0.9, derived from the logarithm of the ratio of the low-E and high-E currents I_H and I_L, is also plotted in Fig. 3a, indicating that the ME-SXR T_e is a sensitive indicator of an impending ELM. For instance, if an active control system would be turned on when the ME-SXR T_e reaches 0.8 keV in Fig. 3a, it would prevent the ELM crash while leaving the plasma unperturbed for most of the ELM cycle. Fig. 3b shows that the ME-SXR signals could provide also a sensitive real-time indicator of the L-H transition using the 'ME-SXR pressure' defined as $I_L \cdot \ln(I_H/I_L)$. The RWM can also be detected with high sensitivity by ME-SXR [5].

With appropriate sensors the ME-SXR technique could thus be of interest for feedback control of the burning plasma. Such sensors could be built using linear arrays as in Fig. 1. Nevertheless for increased immunity to the harsh reactor environment it is of interest to develop designs that can provide much larger signals. Such a design is proposed in Fig. 4a, using continuous 'bi-cell' SXR sensors similar to those used for industrial machine control [9]. The H-mode edge casts an X-ray shadow on the sensor, whose position can be accurately measured using the sum and difference of the bi-cell signals for a precise, non-magnetic plasma position measurement. Fig. 4b shows simulated sensor signals for a typical pedestal emissivity profile, indicating a linear dependence of the signal on the plasma position. In addition, as shown by plots for different pedestal widths, the position signal is little dependent on details of the pedestal profile. Moreover, as sketched in Fig. 4a, two such bi-cells filtered for 'high' and 'low' X-ray energy could be combined to make a ME-SXR position, ELM and RWM sensor. ELM and RWM sensing could be done using for instance the ratio of the 'high' and 'low' position signals. Lastly, a continuous bi-cell sensor would collect much more plasma radiation than one pixel in a 1-D array, allowing using for X-ray sensing radiation-resistant detectors, such as for instance the metal film bolometers developed for ITER [10].

The work at the Johns Hopkins University was supported by US DOE Grants DE-FGO2-86ER53214 and DE-S0000787. The work at PPPL was supported by US DOE Contract DE-AC02-09CH11466.

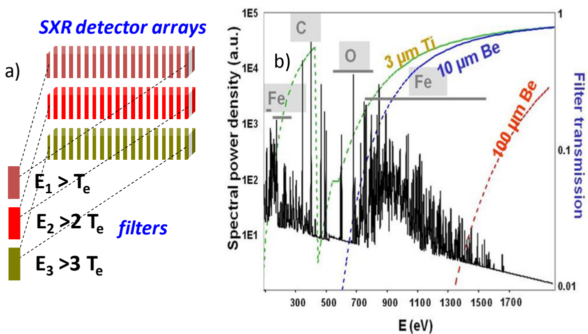

Fig. 1 a) Layout of ME-SXR diagnostic.
b) Computed spectrum of 1 keV plasma with 1.5%C, 0.25% O, and 0.02% Fe impurity; also shown the transmission of ME-SXR filters on NSTX.

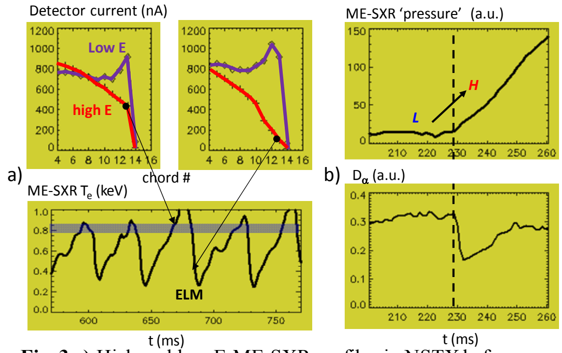

Fig. 3 a) High and low-E ME-SXR profiles in NSTX before and after Type-I ELM and history of 'ME-SXR T_e' at r/a=0.9.
b) Time history of 'ME-SXR pressure' at r/a=0.9 during L-H transition in NSTX. Also shown the D_α signal.

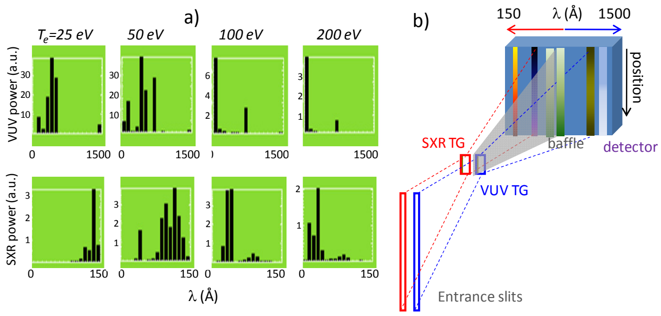

Fig. 2 a) VUV and SXR spectra of plasma with 4% C and 0.8% Ne, at T_e from 25 to 200 eV.
b) Layout of dual grating TGIS diagnostic.

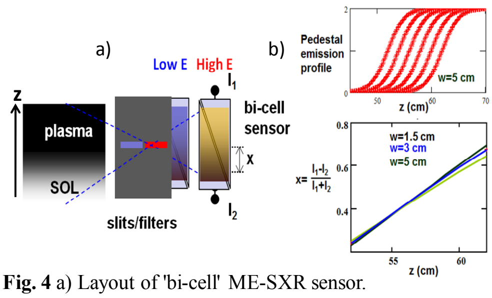

Fig. 4 a) Layout of 'bi-cell' ME-SXR sensor.
b) Computed dependence of bi-cell sensor signal on plasma position (bottom), for an H-mode like pedestal emission profile having width w=5 cm (top). Also shown the sensor signals for different pedestal widths.

1. D J Clayton, K Tritz, D Stutman, D Kumar and M Finkenthal, P1.134 this conference.
2. D Kumar, D Stutman, M Finkenthal, D J Clayton, K Tritz, R Bell, B LeBlanc, P4.047 this conference.
3. D Kumar, D Stutman, K Tritz, M Finkenthal, C Tarrio, S Grantham *Rev. Sci. Instrum.* **81** 10E507 (2010)
4. L Delgado, D Stutman, K Tritz, M Finkenthal et al *Nucl. Fusion* **49** 085028 (2009)
5. L Delgado, D Stutman, S Sabbagh, et al, *Plasma Phys. Control. Fusion* **53** 035005 (2011)
6. K Tritz, S Kaye, R Maingi, S Sabbagh, D Stutman, R Bell, L Delgado et al *Phys. Plasmas* **15** 056119 (2008)
7. K Tritz, D Stutman, L Delgado-Aparicio, M Finkenthal, R Kaita and L Roquemore *Rev. Sci. Instrum*. **81** 10E502 (2010)
8. A E Costley, *IEEE Transactions on Plasma Science* **38**,2934 (2010)
9. E. Derenzo, W. W. Moses, H. G. Jackson, et al., IEEE Trans. Nucl. Sci. **36**, 1084 (1989)
10. H Meister, T Eich, N. Endstrasser, L. Giannone, et al *Rev. Sci. Instrum*. **81**, 10E132 (2010)